Effect of added monovalent electrolytes on the myelin formation from charged lipids

Meiyu Lin [a], Li Li [b], Feng Qiu [a], Yuliang Yang [a],*

[a] The Key Laboratory of Molecular Engineering of Polymers, Ministry of Education, Department of Macromolecular Science, Fudan University, Shanghai 200433, China
[b] The Centre of Analysis and Measurement, Fudan University, Shanghai 200433, China

ARTICLE INFO

ABSTRACT

The effect of added monovalent electrolytes on the myelin formation of cardiolipin is investigated by optical microscopy observations. The results show that the myelin formation strongly depends on the concentration rather than the type of electrolytes. Myelin figures are observed only in a certain concentration range of electrolytes, and the diameter of the myelin figures decreases with increasing of the electrolyte concentration. Furthermore, the theoretical model of myelin formation for the neutral lipids developed by Huang–Zou–Witten [J.R. Huang, L.N. Zou, T.A. Witten, Eur. Phys. J. E. 18 (2005) 279–285] is extended to the charged membrane system by taking into account the electrostatic interaction to understand the mechanism of myelin formation. The theoretical results well produce our experimental results.

1. Introduction

Amphiphilic molecules such as surfactants and lipids can assemble into a variety of microstructures in excess water. One of the structures is myelin figure consisting of a large number of concentric cylindrical bilayers separated by thin hydration layers [1]. There are several methods in experiments to produce myelin figures and one of the most common method is so-called contact experiment. When dehydrated lump of amphiphiles is contacted with water at temperatures high enough so that the bilayers are in fluid state, lots of myelin figures are immediately grown out from the lump–water interface [1,2–9]. Recently, it was reported that myelin figures can also be produced by immersion-and-puncture or drying drop experiment. By immersing vapor-annealed lipid deposit in water and then puncturing the well-ordered bilayer stack on the deposit surface with a sharp needle [10,11], myelin figures were found growing slowly in length from the damaged site. While drying drop experiments generate myelin figures by dehydrating a vesicle [12]. With evaporating a drop of dilute suspension of lipid vesicles on a glass slice, many pancake-like multilamellar disks will develop at the drop's perimeter and further spread inward from the perimeter. During this process, some of these disks undergo structure transformations to form myelin figures from their edges of the disks [12]. In order to theoretically explain the formation of myelin figures via the dehydration process, Huang et al. [12] proposed an argument based on the simple

geometric calculation and revealed that the formation of myelin is induced by the reduction of bilayer repulsions which exceed the gain in the curvature energy due to the increase of bilayer repeat spacing. This theory has successfully predicted the degree of dehydration required to favor myelin figures over the flat lamellae.

Myelin formation from charged surfactants or charged lipids in electrolyte solutions is even more interesting since charged lipids constitute a substantial part of bio-membrane and play an important role in many physiological processes and chemical reactions of vital phenomena [13]. The ubiquitous nature of electrolyte in physiological environment of bio-membranes is also well documented. Although myelins can also form by bringing brine [14] or para-toluene sulfonic acid (PTS) [15] solution contacted with anionic surfactant sodium bis (2-ethylhexyl) sulfosuccinate (AOT) [14,15], myelin formation in charged surfactants is attributed to the wide miscibility gap between lamellae and micelles. In addition, Telkes and Pencl [7] reported the myelin growth from lipid mixtures in various salt solutions in 1933. They found that no myelin growth took place in the concentrated salt solutions, while with increasing dilution the growth reached a maximum and slightly decreased again with greater dilution. Unfortunately, to our knowledge, very limited investigations on the myelin formation in charged lipid systems have been reported.

In this paper, we systematically study the effect of added monovalent electrolytes on myelin formation using cardiolipin, which is a dimeric phospholipid with two negative charges at neutral pH [16], and exclusively exists in bacterial and mitochondrial-membranes. In our experiments, myelin figures are generated by contacting monovalent electrolyte water solution with dried lipid

* Corresponding author. Fax: +86 21 65642867
E-mail address: yuliangyang@fudan.edu.cn (Y. Yang).

lump. In particular, the effects of the type and concentration of monovalent electrolyte on myelin formation are investigated. The observations reveal it is not the ion type but the concentration of electrolytes significantly affects myelin formation. Moreover, myelins occur only in a certain range of electrolyte concentrations and its outer diameter decreases with an increase in the electrolyte concentration. Our experiments are consistent with modified Huang–Zou–Witten's theory [12] by taking into account the electrostatic repulsion between charged bilayers.

2. Materials and methods

2.1. Materials

Cardiolipin sodium salt from bovine heart, with about 98% chemical purity and dissolved in methanol (4.7% concentration), was obtained from Sigma. Cesium chloride (CsCl), tetramethylammonium chloride ($(CH_3)_4NCl$), and tetraethylammonium chloride ($(C_2H_5)_4NCl$), with chemical purity $\geqslant 98\%$, were obtained from Aldrich. NaCl, KCl, and NH_4Cl are analytical grade and were supplied by Shanghai Xingao Chemial Reagent Co., LTD. of China. All above agents were used without further purification.

2.2. Preparation of samples

Methanol was removed from purchased cardiolipin solution first by putting the assigned amount solution in vacuum oven and then the dried-cardiolipin was re-dissolved in chloroform/methanol (9:1 v/v) to reach the concentration of 10.0 mg/ml, which was stored at $-20\,°C$ for later use. A droplet of this lipid solution (1 µl) was deposited on the center of a pre-warmed glass slice. The slice was kept in vacuum oven at $40\,°C$ for 2 h to remove remained solvents and then was transferred to the heating stage of microscope at $40\,°C$. The temperature of the stage was cooled down to $25\,°C$ at a rate of $20\,°C/min$. After a while, a drop of distilled water or electrolyte solution about 2 µl was placed on the dry film. Immediately, the changes in the water–lipid droplet were observed and recorded by the CCD camera.

2.3. Optical microscopy observations

All observations were made under a Microscope (BX51, Olympus, Japan) with a $50\times$ semi-achroplane objective (NA is 0.5, working distance is 10.6 mm), which is equipped with a heating stage ($\pm 0.1\,°C$ accuracy, THMS600, Linkam, England). The evolution of samples in solutions were recorded by a CCD camera (Pixelink, Linkam, England) and analyzed by software Linksys32DV (Linkam, England).

3. Theoretical calculation background

In our contact experiments, electrolyte solution is contacted with concentrated surfactants. Immediately upon the contact, lamellar structures occur at the interface [2,14] and myelin figures are found at suitable electrolyte concentrations. If we consider the whole lamellar stacks as a closed system, the area and occupied volume of the membranes and inter-bilayers water can be considered constant. The simple geometric calculation proposed by Huang–Zou–Witten (HZW) [12] originally for the neutral lipids is extended to understand the myelin formation of charged lipids with added salts solution by taking into account the electrostatic interactions. HZW model [12] attributes the myelin formation from dehydrating flat disk spontaneously to the increase of the bilayer repeat space, favoring the free energy.

In HZW's model, the stability of myelins vs. flat bilayers is determined by comparing the calculations of the free energy including inter-bilayer interaction energy and curvature energy [12,17]. For convenience, only consider the myelin figures with large aspect ratio and ignore the contributions of the end caps of myelin and Gaussian curvature to the curvature energy [12]. Supposing a myelin consisting of N concentric, uniformly spaced bilayer cylinders, the curvature energy per unit area of bilayers E_1 is given by:

$$E_1 = \frac{\kappa_C}{N^2 D_m^2} \ln(2N - 1) \tag{1}$$

where D_m is the bilayer repeat space of myelin, the radii of the innermost cylinder R_i is set as $D_m/2$ for calculation simplicity, which is proven that freeing these two constraints (i.e., allowing D_m to be non-uniform or R_i to vary can only lower the myelin energy further) would not weaken the proposed mechanism for myelin formation [12]. The spontaneous curvature of the lipid is set as zero. κ_C is the effective bending modulus for charged membrane, which can be separated into two parts, namely, $\kappa_C = \kappa_{intr} + \kappa_{el}$, where κ_{intr} is the intrinsic bending modulus, and κ_{el} is the electrical bending modulus [18–20]. In the intermediate region of Poisson–Boltzmann theory [18,21], $\kappa_{el} \sim T\lambda_D/l_B \sim \lambda_D$, where T is the experimental temperature, λ_D is Debye–Hückel screening length dependent on the salt concentration, l_B is the Bjerrum length ($l_B \simeq 0.7$ nm for water). In this paper, we set the bending rigidity $\kappa_{intr} = 1.61 \times 10^{-19}$ J and $\kappa_{el} = 0.15 \times 10^{-19}$ J when $\lambda_D = 0.80$ nm [22,23], and the electrostatic bending rigidity for other λ_D (corresponding to various salt concentration values) is evaluated according to the relationship of $\kappa_{el} \sim \lambda_D$.

The inter-bilayers interaction energy per unit bilayer area E_2 is given:

$$E_2 = -\int_\infty^{d_w} d(d_w)P(d_w) \tag{2}$$

For charged flat membrane, the inter-bilayers interactions include three contributions, namely van der Waals attraction, hydration repulsion and electrostatic repulsion [21,24]. The total inter-bilayer interactions per unit bilayer area $P(d_w)$ is thus the sum of these three parts:

$$P(d_w) = P_{vdw}(d_w) + P_h(d_w) + P_{el}(d_w) \tag{3}$$

$$P_{vdw}(d_w) = -\frac{H}{6\pi}\left[\frac{1}{d_w^3} - \frac{2}{(d_w + d_l)^3} + \frac{1}{(d_w + 2d_l)^3}\right] \tag{4}$$

$$P_h(d_w) = P_{h0}\exp(-d_w/\lambda_h) \tag{5}$$

$$P_{el}(d_w) = P_{el0}\exp(-d_w/\lambda_D) \tag{6}$$

where $P_{vdw}(d_w)$, $P_h(d_w)$ and $P_{el}(d_w)$ are the pressures per unit area representing van der Waals attraction interaction, hydration repulsion and electrostatic repulsion, respectively. H is the Hamaker constant, d_w is the thickness of water layer between two bilayers, and d_l is the bilayer thickness. In Eq. (5), P_{h0} is the amplitude and λ_h is the decay length of the hydration pressure. Eq. (6) describes the effect of electrostatic repulsion interactions, where P_{el0} is the amplitude of electrostatic repulsion and λ_D is Debye–Hückel screening length. Electrostatic interactions are exponentially screened on the length scales larger than λ_D, which depends on the concentration of electrolytes. For example, the concentration range occurring myelin figures in our experiments lies in 0.005–0.375 mol/L NaCl (or KCl and CsCl), and Debye–Hückel screening length λ_D is estimated as in the range of 4.31–0.50 nm according to $\lambda_D = 0.305n_0^{-1/2}$ with n_0 the concentration of the electrolyte [21,25]. We should note that this is larger than the typical Gouy–Chapman length $b \approx 0.15$ nm for charged
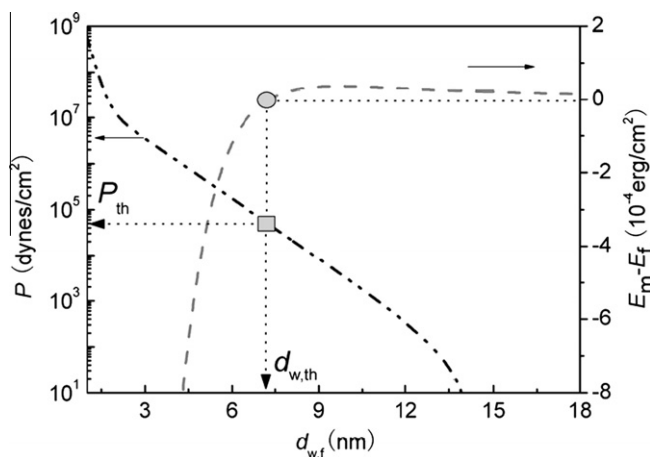
Fig. 1. Calculated free energy difference between flat bilayers and myelins and inter-bilayers pressure as a function of water layer thickness of flat bilayers.

Fig. 3. Myelin diameter vs. NaCl concentration. The error bar indicates standard deviations.

lipids [25,26]. The Gouy–Chapman length b characterizes the thickness of the diffusive counterion layer close to the membrane surface, which is given by $b = 2\varepsilon_0\varepsilon_w k_B T/(q|\sigma|)$ [25], where the vacuum permittivity is $\varepsilon_0 = 8.9 \times 10^{-12} F/m$, the dielectric constant of the aqueous solution is $\varepsilon_w = 80$, $k_B = 1.38 \times 10^{-23}$ J is the Boltzmann constant, the temperature is set as $T = 298$ K, $q = 1.6 \times 10^{-19}$ C is the unit charge, σ is the surface charge distribution assumed to be negative. By assuming complete dissociation, the area per phospholipid head group is about 6.6×10^{-19} m² for phosphatidyl-serine (PS) [25,26]. Moreover, we expect the water layer thickness, d_w, after hydration is generally larger than the λ_D. Hence, λ_D in our system lies in $b \ll \lambda_D \ll d_w$, namely in the intermediate region of Poisson–Boltzmann theory, and electrostatic repulsion pressure can be described by Eq. (6) [21,25].

In the constraint of conservation of the volume V, bilayer area A and number of bilayers N, the bilayer repeat space for myelins D_m and for flat disks D_f is related by $D_m = (1 + 1/(2N - 1))D_f > D_f$, so that the water layer thickness of myelins $d_{w,m}$ is $d_{w,m} = (1 + 1/(2N - 1))d_{w,f} + d_l/(2N - 1)$, where $d_{w,f}$ and d_l are the water layer thickness of flat multilamellar disk and the bilayer thickness respectively ($D_m = d_{w,m} + d_l$ and $D_f = d_{w,f} + d_l$). Because d_l is roughly constant during the flat layers to myelins structure transformation [12,17], the water layer thickness will increase when a multilamellar disk is transformed into a myelin. In this situation, inter-bilayers repulsion interactions should decrease according to Eq. (3). Therefore, if decreasing of inter-bilayers repulsion energy in the case of charged membranes is dominant over the curvature energy of forming myelins, myelins will form instead of flat membranes to reduce the free energy of the system.
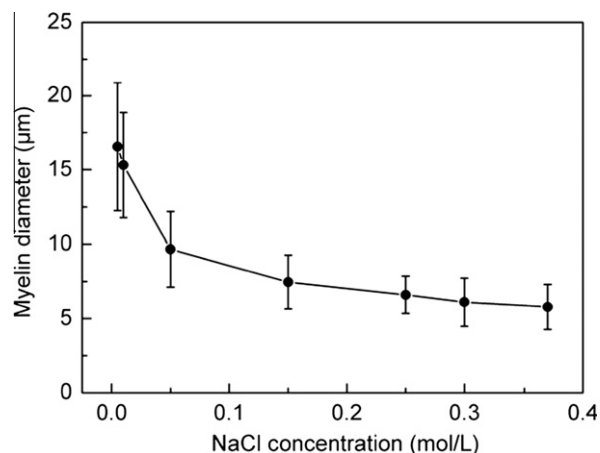
Subsequently, we can compare the free energy of flat bilayers $E_f(E_f = E_2(d_{w,f}))$ with that of myelin structures $E_m(E_m = E_1(d_{w,m}) + E_2(d_{w,m}))$ under the above conservation assumptions. In the calculation, the hydration repulsion is set as $P_h(d_w) = 10^{11} \exp(-d_w/1.93)$ dynes/cm² [27,28], the amplitude of the electrostatic pressure is $P_{el0} = 7 \times 10^7$ dynes/cm² [17], $H = 1 \times 10^{-14}$ dynes·cm [17,28] and $d_l = 3.50$ nm [17]. $\lambda_D = 1.00$ nm (corresponding to the concentration 0.093 M); $N = 400$ (the average diameter of myelin is about 8 μm in Fig. 3). Fig. 1 shows that the energy difference between flat bilayers and myelin structures ($E_m - E_f$) increases from negative to positive as the water layer thickness enlarges. Here the water layer thickness of flat bilayers $d_{w,f}$ is chosen as the X axis since $d_{w,m}$ has a fixed relationship with $d_{w,f}$ as mentioned above. For the convenience of discussing flat bilayers-myelins transition, we define the state ($E_m - E_f = 0$) as the threshold point, where the free energy of the flat bilayers is equal to that of the myelins and the corresponding water layer thickness and inter-bilayers pressure are called critical $d_{w,th}$ and P_{th}, respectively. When $d_{w,f}$ is smaller than the $d_{w,th}$ or $P(d_{w,f})$ is larger than the P_{th}, the free energy of myelin figures is smaller than that of flat bilayers, and thus myelin structures will be more stable than flat lamellar structure. On the contrary, when $d_{w,f}$ is larger than the $d_{w,th}$ or $P(d_{w,f})$ is smaller than the P_{th}, the myelin would not form spontaneously.

4. Results and discussion

We should mention in advance that the myelin formation from charged lipids with added salt solution can only be achieved by the immersion or contact experiments as the dehydration process will
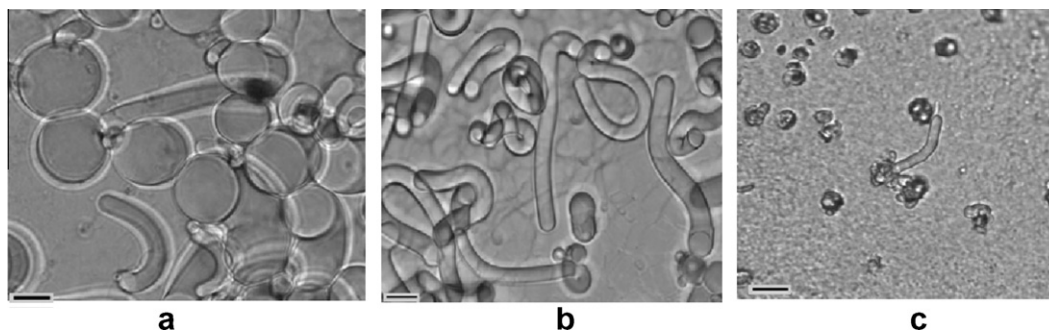
Fig. 2. Effect of NaCl concentration in hydrating solutions on the myelin formation from negatively charged cardiolipin. The scale bars represent 20 μm. (a) Myelin figures with onion-like structures at 0.010 M NaCl solution; (b) myelin figures at 0.150 M NaCl solution and (c) thinner myelin figures with some irregular structures at 0.370 M NaCl solution.

alter the salt concentration during the evaporation of water. In this paper, myelin figures are prepared by contact experiments.

To investigate NaCl concentration on the myelin formation, Fig. 2 presents the myelin figures formed in three different concentrations of NaCl solutions. At middle concentration solution of 0.150 mol/L NaCl in Fig. 2b, well-shaped myelin figures with large aspect ratio, i.e., $L \gg R_0$ (where L and R_0 are the length and radius of myelin figures, respectively), are the dominant structures and their diameters are relatively even distributed. At higher NaCl concentration, e.g., 0.370 mol/L, myelin growth was inhibited, and only a small amount of thinner myelin figures occurs in Fig. 2c. At lower NaCl concentration, e.g., 0.010 mol/L in Fig. 2a, besides large aspect ratio myelin figures, some myelin figures but with small aspect ratio along with onion-like structures are found. Similar experiments with charged lipid system also show that relatively concentrated salt solution retarded myelin growth, while more dilute solutions stimulated it [7]. We should note that the roots of the myelin and onion-like structures in our experiments do not move at all when we stir the surrounding water in the surface of initial surfactants by a needle. Therefore myelins and onion-like structures shown in Fig. 2 are not detached from the initial surfactant phase but with the roots of myelins and onion-like structures connected with the initial surfactant phase.

To further quantify the effect of electrolyte concentration on the myelin diameter, plot the diameter of myelin figures as a function of NaCl concentration in Fig. 3. The diameter of myelin figures is averaged over 100 typical myelin figures. It is indicated that with the increasing of NaCl concentration, the average diameter of myelin figures decays quickly when NaCl concentration is less than 0.100 mol/L, and decreases slowly above 0.100 mol/L. The diameter of the myelin is proportional to the number of the bilayer N and bilayers repeating space if the water core is ignored. It is obvious that the whole stack of bilayers transforms into one myelin along the height shown in Fig. 2b. Therefore, we suggest that the bilayer number of myelins N is the same as that in the flat membrane, which is determined by preexisting structures in the dry lipid film dependent on the experimental method and parameters [12]. Because we adopt the same experimental procedure to prepare the dry lipid film, the bilayer number N is approximately regarded as constant if we average out the randomness. So the diameter of the myelins is mainly influenced by the bilayers repeating space which is governed by the inter-bilayers interactions. With the NaCl concentration increasing, the Debye–Hükel screening length λ_D decreases. Consequently, the electrostatic repulsion interactions between the neighbouring membranes according to Eq. (6) weaken leading to the decrease of water layer thickness and the decrease of myelins diameter accordingly, although the membrane thickness remains almost constant. Similar results has also been drawn from the theoretical analysis of Komura et al. [25], who focused on the phase behavior of the aqueous solution of charged lipid bilayer membranes forming a lamellar structure in the presence of added electrolytes.

To illustrate the influence of the nature of added electrolytes on the results shown in Fig. 2, five different monovalent chlorides including KCl, CsCl, NH₄Cl, (CH₃)₄NCl, and (C₂H₅)₄NCl aqueous solutions are employed to hydrate cardiolipin lump. The results show that the morphologies for various added electrolytes are very similar and assembling structures of charged lipids strongly depend on electrolyte concentration of the solution. Myelin figures occur only in a certain range of electrolyte concentrations for all chlorides. In the solution with electrolyte concentration below the lower limit, only onion-like morphologies can be observed. With the concentration above the upper limit, only some irregular structures emerge. The detailed available concentration ranges and the upper/lower limits of concentrations for myelin existence are summarized in Table 1. We note that the reason for the 'gap' existing between the different regimes in Table 1 is the determination of the boundary being ambiguous.

Table 1
The effect of concentrations of added monovalent salts on the myelin formation from charged lipids.

Electrolyte species	Lower limit of concentrations[a] (mol/L)	Concentration range available for myelin formation[b] (mol/L)	Upper limit of concentrations[c] (mol/L)
NaCl	<∼0.003	0.005–0.375	>0.550
KCl	<∼0.003	0.005–0.375	>0.550
CsCl	<∼0.003	0.005–0.375	>0.550
NH₄Cl	<∼0.003	0.005–0.400	>0.850
(CH₃)₄NCl	<∼0.003	0.005–0.700	>1.100
(C₂H₅)₄NCl	<∼0.003	0.005–1.200	>1.500

[a] Below this salt concentration, only the onion-like morphologies are observed.
[b] Within this salt concentration range, large amount of myelin figures can be observed.
[c] Higher than this salt concentration, only some irregular structures are observed.

From Table 1, it is clear that the ranges of the salt concentrations suitable for myelin formation are same for the smaller species, such as NaCl, KCl and CsCl, and gradually toward higher concentrations with the increasing of the cationic group sizes such as NH₄Cl, (CH₃)₄NCl, and (C₂H₅)₄NCl. That is, for smaller size species (NaCl, KCl and CsCl), the available concentration range for myelin formation is 0.005–0.375 M, and is insensitive to the cationic types. However, for the bulkier electrolytes, NH₄Cl, (CH₃)₄NCl and (C₂H₅)₄NCl, the concentration ranges suitable for myelin growth tend to higher concentrations, such as 0.005–0.400, 0.005–0.700 and 0.005–1.200 mol/L, respectively. The slight difference between these two concentration ranges available for myelin formation may result from the difference of effective electrostatic screening effects between the small and large size ionic groups. Podgornik et al. [29] studied the polymer-condensed arrays of parallel DNA double helices in monovalent salt solutions. In their measurement of the mean repulsive force and lateral fluctuations between the arrays, they found that when the salt concentration was raised from 0.4 to 2.0 mol/L, the measured Debye–Hükel screening length of the smaller cationic species NaCl decreased from 0.96 nm to 0.64 nm; while those of the bulkier cationic species, (CH₃)₄NCl and (C₂H₅)₄NCl, only decreased from 0.80 and 0.78 to 0.73 nm, respectively. Their results suggested that in comparison to Na⁺, the larger salt ions adsorb and condense very poorly to the surface, leaving more DNA phosphates unneutralized.

For charged lipids, the added electrolyte concentration will influence Debye–Hückel screening length λ_D which further affects the inter-bilayers electrostatic interactions according to Eq. (6). As a result, the threshold thickness of water layers $d_{w,\text{th}}$ and the corresponding P_{th} are strongly influenced as mentioned above in the section of theoretical calculation background. Fig. 4 shows the calculated values of P_{th} and $d_{w,\text{th}}$ change with different Debye–Hückel screening length λ_D (corresponding to salt concentration). It is showed that $d_{w,\text{th}}$ decreases with the salt concentration increasing (λ_D decreasing), while P_{th} increases with the salt concentration increasing (λ_D decreasing).

The lipid used in our experiments is cardiolipin sodium salt, which is negatively charged lipid at neutral pH [16]. So when water penetrates lipid lamellae, the electrolyte ion (Na⁺) would be bound to both sides of charged bilayers, schematically shown in Fig. 5a. Moreover, the thickness of water layers between the bilayers becomes quite large from the beginning. It implies that this minimum water layer thickness between neighbouring bilayers is at least $2D_{\text{Na}^+}(=1.44 \text{ nm})$ according to the steric repulsion (D_{Na^+} defined as the diameter of hydrated Na⁺ is 0.72 nm [30–32]). Moreover, Sein and Engberts [33] suggested that besides water molecules, screening ions such as Na⁺ and the corresponding disso-
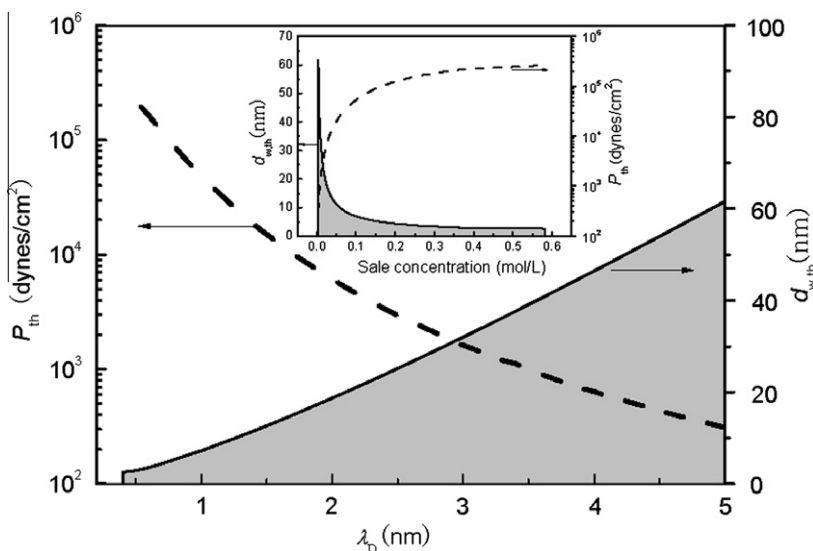
Fig. 4. The threshold water layer thickness $d_{w,th}$ and pressure P_{th} for the flat membrane as a function Debye–Hückel screening length λ_D (corresponding to salt concentration). In the shaded area where $d_{w,f} < d_{w,th}$ ($P > P_{th}$) and thus the flat membrane is unstable against the myelin formation. In the calculation, $N = 400$, other parameters are the same as those in Fig. 1.

ciated counterion Cl$^-$ would penetrate the membrane from the lamellar roots [2]. The diameters of the water molecule and hydrated Cl$^-$ are 0.40 nm and 0.66 nm [30–32], respectively. So Na$^+$ and the dissociated counterion Cl$^-$ and water molecules, possibly occupy volume, schematically shown in Fig. 5b.

Therefore, the actual minimum water layer thickness may be larger than 2.16 nm equivalent to the thickness of $3D_{Na^+}$ due to the repulsion of like charges. It is interesting to note that this value is very close to the threshold water layer thickness $d_{w,th}$ namely 2.91 nm at the electrolyte concentration of 0.372 M shown in Fig. 4. This implies that the water layer thickness may be larger than the threshold water layer thickness $d_{w,th}$ at higher electrolyte concentrations from the beginning when the electrolyte solution is contacted with the dried lipid lump. This is the reason why nearly no myelin figures are observed when the electrolyte concentration is larger than 0.375 M, requiring rather low value of $d_{w,th}$. Another reason may be related to the fast lamellar swelling rate. The driving force for the swelling of a lamellar phase is the net repulsions between the inter-bilayers [34,35], which is always very strong during the whole process of the water layer thickness $d_{w,f}$ enlarging to $d_{w,th}$ at relatively high electrolyte concentrations, shown in Figs. 1 and 4. Therefore, the water layer thickness may be exceeds $d_{w,th}$ before the myelin formation for the quickly lamellar swelling and myelin figures would not be observed in this case.

On the other hand, when the electrolyte concentration is decreased to 0.005 M, in our experiments, the formed myelin figures are normally with small aspect ratios and even in the extreme, onion-like shapes occur. It is suggested that at low salt concentrations, due to feelable static repulsion screening the static repulsion is so strong that the water layer thickness becomes relatively large and the diameter of the cylinders becomes large accordingly. However, the myelin growth rate decreases quickly with the decreasing of NaCl concentration as shown in Fig. 6. Therefore, in this case such as the salt concentration less than 0.005 M the myelin growth can be neglected. This results in relatively small ratio of the length to diameter of the cylinder. Moreover, if the myelins or cylinders are transformed into concentric spheres or onion-like shapes, the bilayer repeat spacing will be further increased and the repulsion energy would further decrease when the cylinder is transformed into spheres or onions according to the relationship between the bilayer repeat spacing of spheres or onions D_O and that of the myelins (or cylinders) $D_O = (1 + 1/2N)D_m$.

The effect of electrolytes on the myelin growth is investigated through analyzing myelin length L (the distance from myelin root to top), as a function of the growth time t at different NaCl concentrations. We average the individual myelin length over 10 measurements at each NaCl concentration and plot the square of averaged myelin lengths L^2 vs. time t, as shown in Fig. 6. The growth is linear and can be simply expressed as $L^2 = k_m t + C$, where
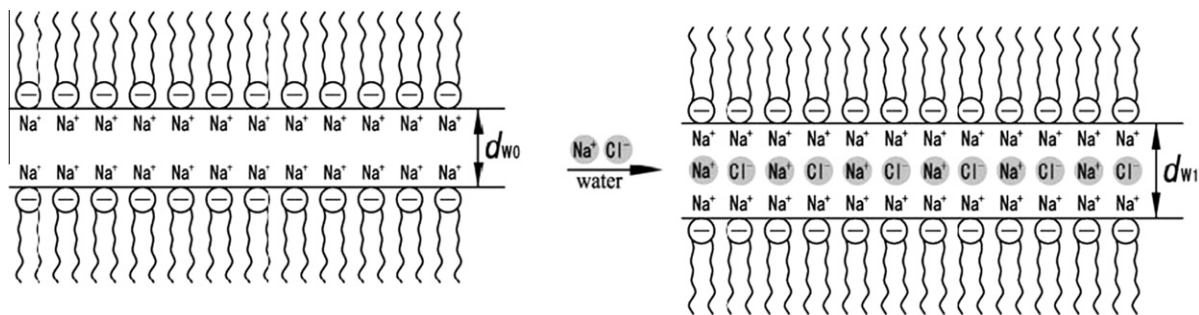
Fig. 5. Schematic drawing of negative charged lipid bilayers in lamellar structure. (a) Before screening ions penetrate the minimum water layer thickness $d_{w0} = 2D_{Na^+} = 1.44$ nm (D_{Na^+} defined as the diameter of hydrated Na$^+$ is 0.72 nm [30–32]); (b) After screening ions penetrate the minimum water layer thickness $d_{w1} = 3D_{Na^+} = 2.16$ nm (the diameter of hydrated Cl$^-$ is estimated as 0.66 nm [30–32], smaller than that of Na$^+$).
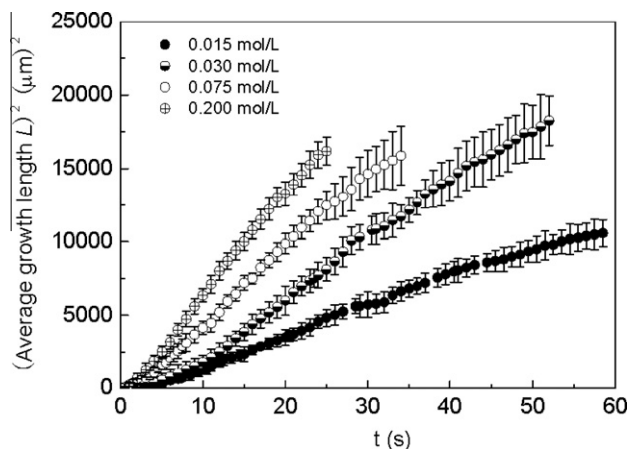
Fig. 6. Plot of square of average myelin length against time in different concentrations of NaCl solution. Each curve has been averaged over more than 10 growing myelin tubes. The figure indicates that the growth law meets $L^2 = k_m t + C$, where k_m represents the growth rate constant. The error bar indicates standard deviations.

k_m represent the growth rate constant. It is clear that the myelin growth represents the pseudodiffusion characteristics, which is similar to that in other system of contact experiments [2,10,15]. Furthermore, the scaling law does not change with the type and concentration of electrolyte. When we replace NaCl with other electrolytes such as KCl, CsCl and $(C_2H_5)_4$NCl, similar results are obtained. It is indicated that myelin growth kinetics is less dependent on the type of electrolyte and the growth rate increases with the electrolyte concentration increasing.

5. Conclusion

In this paper, the effect of monovalent electrolytes on the myelin formation from negative charged lipids is systematically investigated. Huang–Zou–Witten [12] theoretical model originally for neutral system is extended to understand the myelin formation by including the electrostatic interaction. The experimental results show that the effect of added monovalent electrolytes on the myelin formation from charged lipids is strongly dependent on the concentration of electrolytes, which mainly influences the screened electrostatic interaction characterized by Debye–Hückel screening length, λ_D. The myelin formation is not sensitive to the specific ion types of added electrolytes. Typical myelin figures are observed only in the intermediate salt concentration regions such as 0.005–0.375 M for small size electrolytes, and the diameter of myelins decays with the electrolyte concentration increasing. In the high concentration region (>0.550 M), the threshold water layer thickness $d_{w,th}$ (when the water layer thickness of flat membrane $d_{w,f}$ is smaller than the $d_{w,th}$, the free energy of myelin figures is lower than that of flat bilayers, leading to more stable myelins compared to flat lamellar structure) is very small. Myelins can not be observed experimentally in this case because the minimum water layer thickness is larger than $d_{w,th}$ due to the steric repulsion between counterions and water. In the low salt concentration region (<∼0.003 M), onion-like figures are observed. This is possibly due to strong repulsions between membranes, and the repulsion energy would further decrease when cylinders (myelins) are transformed into spheres or onions with the bilayer repeat spacing further increasing. The relationship between the average myelin length L and the growth time t satisfies $L^2 = k_m t + C$, where k_m represents the growth rate constant. Moreover, this relationship does not change with the salt type and concentration, but the growth rate constant k_m increases with the salt concentration increasing.

References

[1] I. Sakurai, T. Suzuki, S. Sakurai, Biochim. Biophys. Acta 985 (1989) 101–105.
[2] M. Buchanan, S.U. Egelhaaf, M.E. Cates, Langmuir 16 (2000) 3718–3726.
[3] A.P. Kennedy, J. Sutcliffe, J.X. Cheng, Langmuir 21 (2005) 6478–6486.
[4] V. Frette, I. Tsafrir, M.A. Guedeau-Boudeville, L. Jullien, D. Kandel, J. Stavans, Phys. Rev. Lett. 83 (1999) 2465–2468.
[5] I. Sakurai, Y. Kawamura, Biochim. Biophys. Acta 777 (1984) 347–351.
[6] I. Sakurai, Biochim. Biophys. Acta 815 (1985) 149–152.
[7] M. Telkes, D. Pencl, Ohio J. Sci. 33 (1933) 85–100.
[8] H. Dave, M. Surve, C. Manohar, J. Bellare, J. Colloid Interface Sci. 264 (2003) 76–81.
[9] R. Taribagil, M.A. Arunagirinathan, C. Manohar, J.R. Bellare, J. Colloid Interface Sci. 289 (2005) 242–248.
[10] L.N. Zou, S.R. Nagel, Phys. Rev. Lett. 96 (2006) 138301.
[11] L.N. Zou, Phys. Rev. E. 79 (2009) 061502.
[12] J.R. Huang, L.N. Zou, T.A. Witten, Eur. Phys. J. E. 18 (2005) 279–285.
[13] M. Langner, K. Kubica, Chem. Phys. Lipids 101 (1999) 3–35.
[14] M. Buchanan, J. Arrault, M.E. Cates, Langmuir 14 (1998) 7371–7377.
[15] M. Haran, A. Chowdhury, C. Manohar, J. Bellare, Colloids Surf. A 205 (2002) 21–30.
[16] Y.S. Tarahovsky, A. Larry Arsenault, R.C. MacDonald, T.J. McIntosh, R.M. Epand, Biophys. J. 79 (2000) 3193–3200.
[17] L.J. Lis, M.M. Mcalister, N. Fuller, R.P. Pand, Biophys. J. 37 (1982) 657–666.
[18] J.L. Harden, C. Marques, J.F. Joanny, D. Andelman, Langmuir 8 (1992) 1170–1175.
[19] P.G. Higgs, J.F. Joanny, J. Phys. 51 (1990) 2307–2320.
[20] S. May, J. Chem. Phys. 105 (1996) 8314–8323.
[21] D. Andelman, Handbook of Biological Physics 1 (1995) 603–641.
[22] J. Song, R.E. Waugh, J. Biomech. Eng. 112 (1990) 235–240.
[23] M. Winterhalter, W. Helfrich, J. Phys. Chem. 96 (1992) 327–330.
[24] E.A. Evans, V.A. Parsegian, Proc. Nat. Acad. Sci. 83 (1986) 7132–7136.
[25] S. Komura, H. Shirotori, T. Kato, J. Chem. Phys. 119 (2003) 1157–1164.
[26] M.E. Loosley-Millman, R.P. Rand, V.A. Parsegian, Biophys. J. 40 (1982) 221–232.
[27] A.C. Cowley, N.L. Fuller, R.P. Rand, V.A. Parsegian, Biochemistry 17 (1978) 3163–3168.
[28] D.M. LeNeveu, R.P. Rand, V.A. Parsegian, Nature 259 (1976) 601–603.
[29] R. Podgornik, D.C. Rau, V.A. Parsegian, Macromolecules 22 (1989) 1780–1786.
[30] J. Sabin, G. Prieto, J.M. Ruso, R. Hidalgo-Alvarez, F. Sarmiento, Eur. Phys. J. E. 20 (2006) 401–408.
[31] J.N. Israelachvili, Intermolecular and Surface Forces, Academic Press, New York, 1991.
[32] A. Cernescu, T. Luchian, Cent. Eur. J. Phys. 3 (2005) 15–24.
[33] A. Sein, J.B.F.N. Engberts, Langmuir 12 (1996) 2924–2931.
[34] A. Sein, J.B.F.N. Engberts, Langmuir 12 (1996) 2913–2923.
[35] P.B. Warren, M. Buchanan, Curr. Opin. Colloid Interface Sci. 6 (2001) 287–293.